DALTON
FULL PAPER

A theoretical analysis of the fundamental stepwise six-electron oxidation of porphyrinogen to porphyrins: the energetics of porphodimethene and artificial porphyrin intermediates †

Paola Belanzoni,[a] Marzio Rosi,[a] Antonio Sgamellotti,*[a] Lucia Bonomo[b] and Carlo Floriani[b]

[a] *Centro di Studio CNR per il Calcolo Intensivo in Scienze Molecolari, c/o Dipartimento di Chimica, Università di Perugia, via Elce di Sotto 8, I-06123 Perugia, Italy. E-mail: marzio@thch.unipg.it; Fax: +39 075 5855606*

[b] *Institut de Chimie Minérale et Analytique, BCH Université de Lausanne, CH-1015, Lausanne, Switzerland*

Received 2nd January 2001, Accepted 6th March 2001
First published as an Advance Article on the web 4th April 2001

Density functional calculations have been carried out on a series of model hypothetical intermediates in the six-electron oxidation of porphyrinogen (5,10,15,20,22,24-hexahydroporphyrin) to porphyrin. Two possible reaction pathways have been investigated: the conventional one, supposed to be followed both in the chemical synthesis and the biosynthesis of porphyrins, and the unconventional one, which has been discovered on studying the oxidation of a stable form of porphyrinogen, namely *meso*-octaalkylporphyrinogen. The energetics of both pathways have fully been investigated for the free porphyrinogen. The conventional route is strongly preferred with respect to the unconventional one. The metal-assisted six-electron oxidation of porphyrinogen to porphyrin was also investigated by density functional calculations on several nickel and cobalt model complexes. The metal does not seem to be able to force the system to follow a different route; the conventional route is even more preferred with respect to the unconventional one.

Introduction

The discovery of artificial porphyrins[1] has suggested the possibility of a different pathway in the six-electron oxidation of porphyrinogen (5,10,15,20,22,24-hexahydroporphyrin) to porphyrin, as depicted in Scheme 1, where pathway **b** is the supposed conventional route, while **a** is the route through the intermediate formation of artificial porphyrins. Although pathway **b** is usually accepted as being followed in the auto-oxidation of *meso*-tetraalkyltetrahydroporphyrinogen, only indirect evidence has been produced so far to support it.[2]

The quite recent investigation both on the metal-assisted and on the metal-free *meso*-octaalkylporphyrinogen (pathway **a** in Schemes 1 and 2) led to the discovery of the two- (**2a** Scheme 1, **6a** Scheme 2) and four-electron (**3a** Scheme 1, **7a** Scheme 2) oxidized forms of the porphyrinogen skeleton, other than the natural porphyrins.[3–6] They derive from an electronic oxidation which does not imply the simultaneous removal of any hydrogen atom in *meso* position. Such oxidized forms contain a cyclopropane functionality (△) which functions as a two-electron shuttle.[7] It should be mentioned that a chemical experimental correlation has been found between the related species of pathways **a** and **b** in Schemes 1 and 2, namely the conversion of **2a** into **2b** (Scheme 1), **6a** into **6b** (Scheme 2), **3a** into **3b** (Scheme 1), and **7a** into **7b** (Scheme 2).

The present paper is focused on density functional calculations on the model compounds depicted in Schemes 1 and 2, in order to understand the energy requirements both for the conventional pathway **b** and the unconventional pathway **a**. The model compounds differ from the experimental ones in the substituents at *meso* positions, since in the former case hydrogens are exclusively used instead of ethyl or other alkyl groups. Such a replacement should not have a relevant influence on the electronic and structural properties of the systems. We used, mainly for comparison, structural parameters for all the compounds in both schemes taken from the corresponding *meso*-alkyl derivatives. In particular, the relationship between the model and the experimental compound has been established.

A parallel investigation on the metal-free (Scheme 1) and on the metal-containing forms (Scheme 2) of the various porphyrinogen-derived species paving the way to porphyrins was undertaken with the purpose to understand the major influence in both selecting the pathway and affecting the thermodynamic stability of the various species.

Computational details

Methods

Density functional theory (DFT), which has been found to be a very cost effective method to study transition metal systems,[8] has been used for the determination of equilibrium geometries and the evaluation of the energetics of all the investigated systems and processes. All the calculations have been performed using the Amsterdam Density Functional (ADF) program.[9–11] The model geometries were optimized in restricted (unrestricted only for the cobalt systems) Kohn–Sham calculations.[12] The Vosko, Wilk, and Nusair parametrization[13] of the exchange and correlation energy of the homogeneous electron gas[14] was employed in the local density approximation, with Becke's gradient correction to the exchange part of the potential[15] and Perdew's gradient correction to the correlation[16] included self-consistently. The ADF program is characterized by the use of a density fitting procedure[9–11] to obtain accurate Coulomb

† Electronic supplementary information (ESI) available: atom numbering scheme for species **6a**, selected bond distances and angles for complex $[Et_8N_4(\triangle)Ni]$ and the model system $[H_8N_4(\triangle)Ni]$ **6a**. See http://www.rsc.org/suppdata/dt/b1/b100044f/

 DOI: 10.1039/b100044f

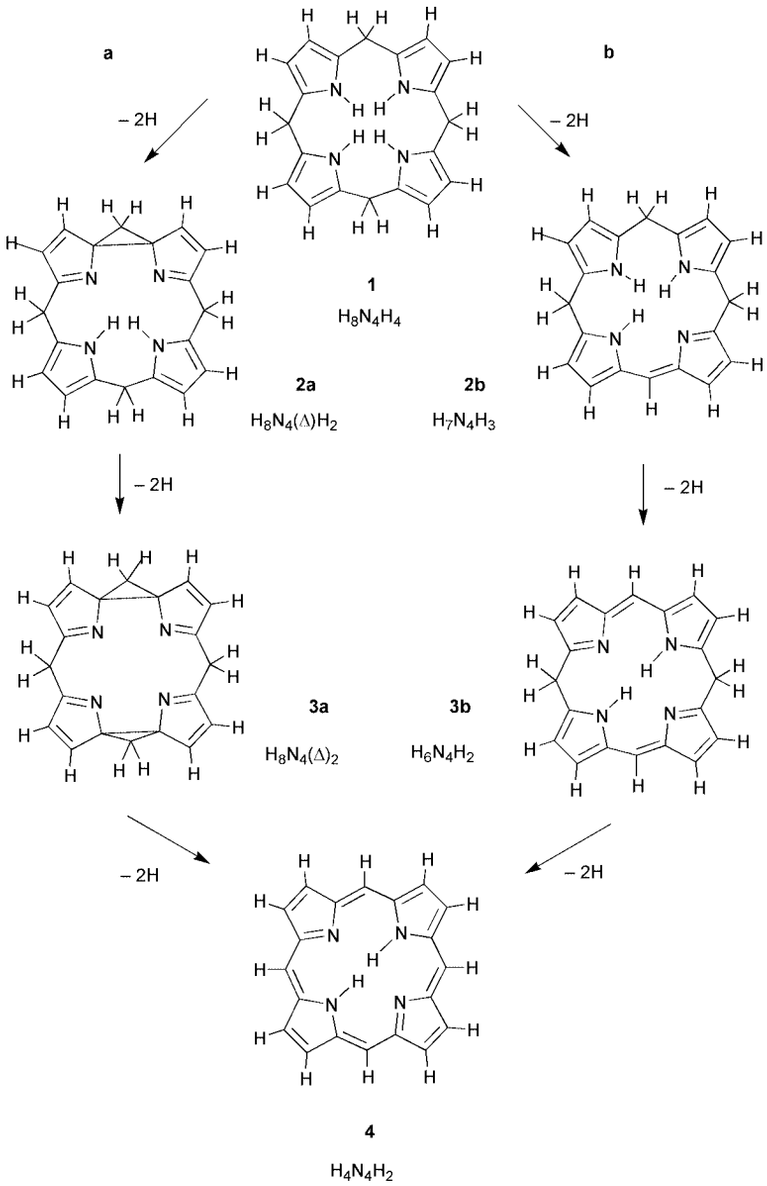

Scheme 1 Unconventional (pathway **a**) *vs.* conventional (pathway **b**) six-electron oxidation of porphyrinogen to porphyrin.

and exchange potentials in each SCF cycle and by the possibility to freeze core orbitals.[9]

Basis sets

Molecular orbitals are expanded in terms of Slater type orbitals (STOs) and the one-electron Kohn–Sham equations[12] are solved self-consistently using highly efficient numerical techniques for integral evaluation.[17,18] The frozen core approximation was used and an uncontracted double-ζ quality basis set plus polarization was employed for H (one polarization 2p STO), C (1s frozen, one polarization 3d STO), and N (1s frozen, one polarization 3d STO), and a triple-ζ plus polarization (one 4p STO) Slater-type orbital basis for the metal, freezing until the 3p shell for Ni and Co.

Model systems and geometry optimization

The geometry of the model systems considered was fully optimized starting from parameters deduced from the available experimental crystal structures. In order to make the calculation feasible, we replaced the alkyl groups (usually ethyl groups) with hydrogens in the *meso*-octaalkylporphyrinogen and its derived systems. The optimization calculations were carried out for each model system using the appropriate symmetry constraint: S_4 for systems **1**, **5** and **8**, C_s for **2a** and **6a**, C_2 for **3a**, **3b**, **7a** and **7b**, C_{2h} for **4** and removing any symmetry constraint for intermediates **2b** and **6b**.

The fully optimized geometries of all the investigated species are available from the authors on request.

Results and discussion

The two parallel pathways (**a** and **b**) displaying the stepwise oxidation of the metal-free porphyrinogen (Scheme 1) and of the metal-containing form (Scheme 2) exemplify the conventional *vs.* the unconventional route leading to porphyrins. The geometries of all the investigated systems have been fully optimized. The optimized structures of species presented in Scheme 1 are shown in Fig. 1, while those of species in Scheme 2 for M = Ni are presented in Fig. 2.

The geometries of the cobalt–porphyrinogen complexes are very close to those of the nickel-porphyrinogen ones and, therefore, are not shown. Only the main geometrical parameters are shown in the figures for clarity. Species **6a**, $[H_8N_4(\triangle)Ni]$,[19] is a model system of the closely related experimental system $[Et_8N_4(\triangle)Ni]$.[4] We can compare therefore the optimized geometry of **6a** with the X-ray geometrical parameters of $[Et_8N_4(\triangle)Ni]$,[4] in order to check the accuracy of the calcu-

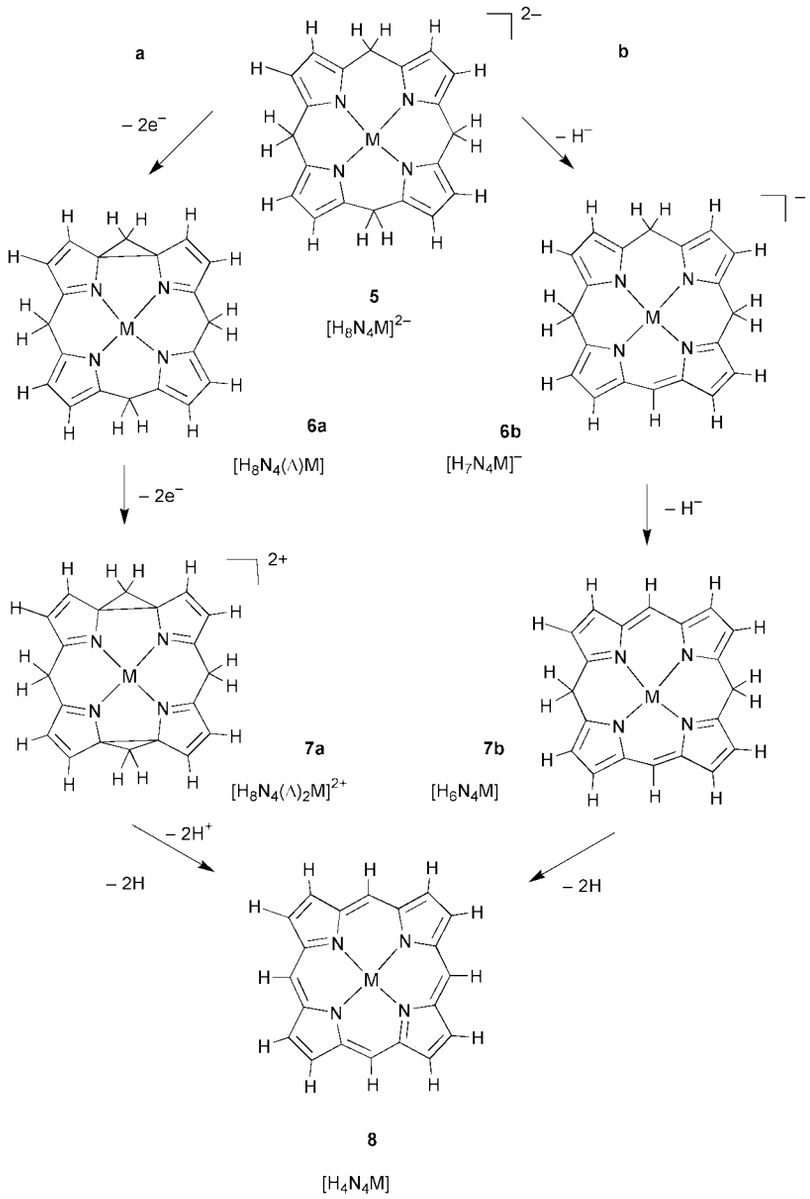

Scheme 2 Unconventional (pathway **a**) *vs.* conventional (pathway **b**) six-electron oxidation of metal–porphyrinogen to metal–porphyrin complexes.

lation. The results are provided as ESI supplementary information. From these results we can notice a very good agreement between calculated and experimental values, that suggests a good quality of the calculation. The only significant deviation is in the dihedral angles between the N_4 core and the pyrrole rings A and B. However this should be due to the replacement of the ethyl groups in *meso* position in the experimental complex with hydrogen atoms in the calculated model system.

Figs. 1 and 2 list the model compounds shown in Schemes 1 and 2, with the calculated C···C distances between the α-carbons of the four pyrroles, which are indicative of the presence or absence of the cyclopropane moiety. The latter functionality is always present in pathway **a** of both schemes, the so-called unconventional route of porphyrinogen leading to porphyrins.

Using the total energies shown in Table 1 we can evaluate the energetics of the conventional and unconventional pathways in Schemes 1 and 2. Let us start with the metal-free molecules shown in Scheme 1. The loss of two hydrogens by the porphyrinogen can lead both to intermediate $H_8N_4(\triangle)H_2$ **2a** or to $H_7N_4H_3$ **2b**. The loss of two more hydrogens by these intermediates can lead to $H_8N_4(\triangle)_2$ **3a** or to $H_6N_4H_2$ **3b**, respectively. Both these intermediates finally can give the porphyrin $H_4N_4H_2$, through the loss of two more hydrogens. We can estimate the thermodynamics of pathways **a** and **b** by considering simply the loss of a hydrogen molecule in each step.

Table 1 Total energies of the investigated systems

Molecule	Symmetry	Ground state		Total energy[a]/eV	
1	S_4	^1A		−280.42	
2a	C_S	$^1A'$		−270.63	
2b	C_1	^1A		−272.33	
3a	C_2	^1A		−260.62	
3b	C_2	^1A		−264.63	
4	C_{2h}	^1A_g		−257.52	
		M = Ni	Co	Ni	Co
5	S_4	^1A	^2A	−271.32	−273.87
6a	C_S	$^1A'$	$^2A'$	−267.91	−270.47
7a	C_2	^1A	^2B	−252.07	−254.66
6b	C_1	^1A	^2A	−268.52	−271.11
7b	C_2	^1A	^2A	−262.75	−265.40
8	S_4	^1A	^2A	−255.70	−258.54

[a] With respect to atoms.

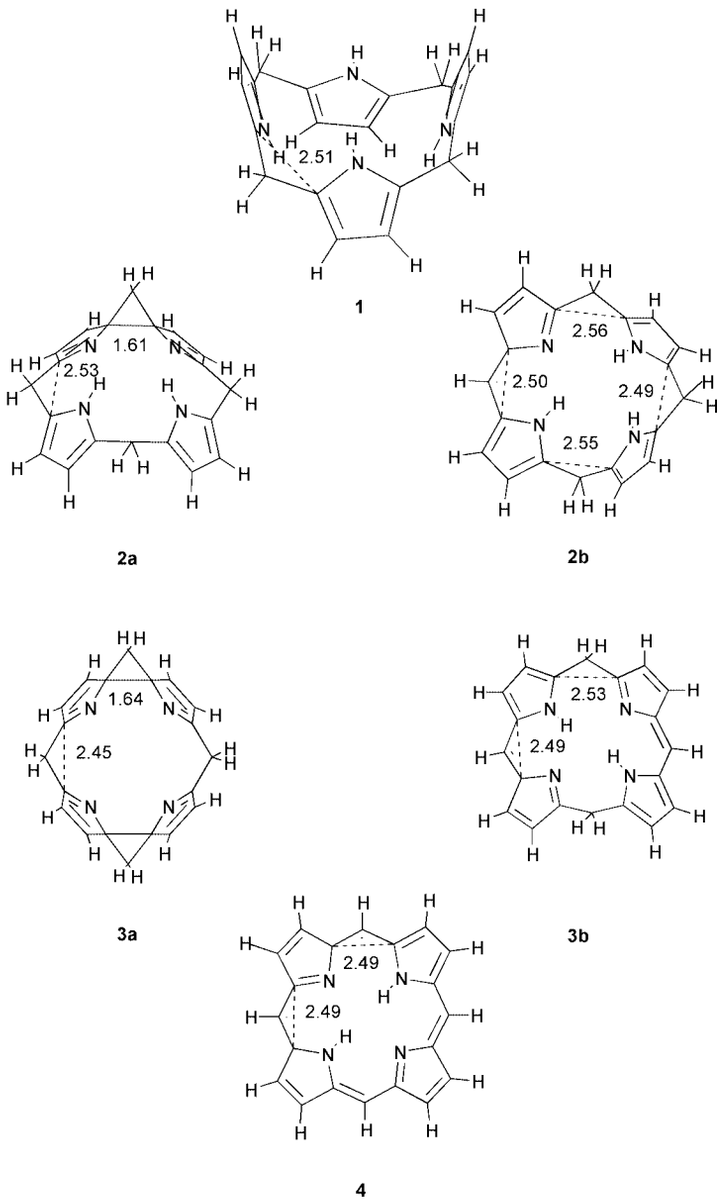

Fig. 1 Optimized structure of $H_8N_4H_4$ (species **1**), $H_8N_4(\triangle)H_2$ (**2a**), $H_7N_4H_3$ (**2b**), $H_8N_4(\triangle)_2$ (**3a**), $H_6N_4H_2$ (**3b**), $H_4N_4H_2$ (**4**). For clarity only the main geometrical parameters are shown. Bond lengths in Å.

Table 2 Energetics for the free ligand unconventional and conventional routes and relative stability of the intermediate species. Energies in kcal mol^{-1}

Step	ΔE
1 ⟶ **2a** + H_2	71
1 ⟶ **2b** + H_2	32
2a ⟶ **3a** + H_2	76
2b ⟶ **3b** + H_2	23
3a ⟶ **4** + H_2	−84
3b ⟶ **4** + H_2	9
Relative stability	
2a ⟶ **2b**	−39
3a ⟶ **3b**	−92

The computed energetics are shown in Table 2 which also gives the relative energies of the related pair of compounds **2a**/**2b** and **3a**/**3b**. We can notice that the intermediates **2b** and **3b** are more stable than the corresponding **2a** and **3a**, and the species **3a** is particularly unstable. In particular species **2b** is computed to be more stable than **2a** by 39.2 kcal mol^{-1}. Species **3b** is computed to be more stable than **3a** by 92.3 kcal mol^{-1}. Moreover, the values of Table 2 suggest that the conventional pathway **b** is preferred, as expected, each step involving almost the same change of energy. On the other hand, the unconventional route **a** proceeds in a more "jumping" way, as the single steps involve quite different changes in energy. In the unconventional route **a** the last step is strongly exothermic (−83.6 kcal mol^{-1}), but it should involve a very high barrier since it requires a strong geometrical rearrangement of the system.

The comparison of the conventional and unconventional pathways is less straightforward when a metal center is present. We have considered the systems shown in Scheme 2, which are all complexes of Ni^{II} or Co^{II}, in order to avoid variations in the oxidation state of the metal. The energetics of pathways **a** and **b** is shown in Table 3. For analogy with the free ligands, we have reported also the relative stability of the intermediates containing the metal, *i.e.* **6a**, **6b** and **7a**, **7b**.

The same trend observed for the metal-free porphyrinogen-derived species, but more amplified, has been found for the metal–porphyrinogen-derived complexes. It should be anticipated, however, that, in the case of forms containing the metal, a major energy factor in the theoretical calculations is certainly

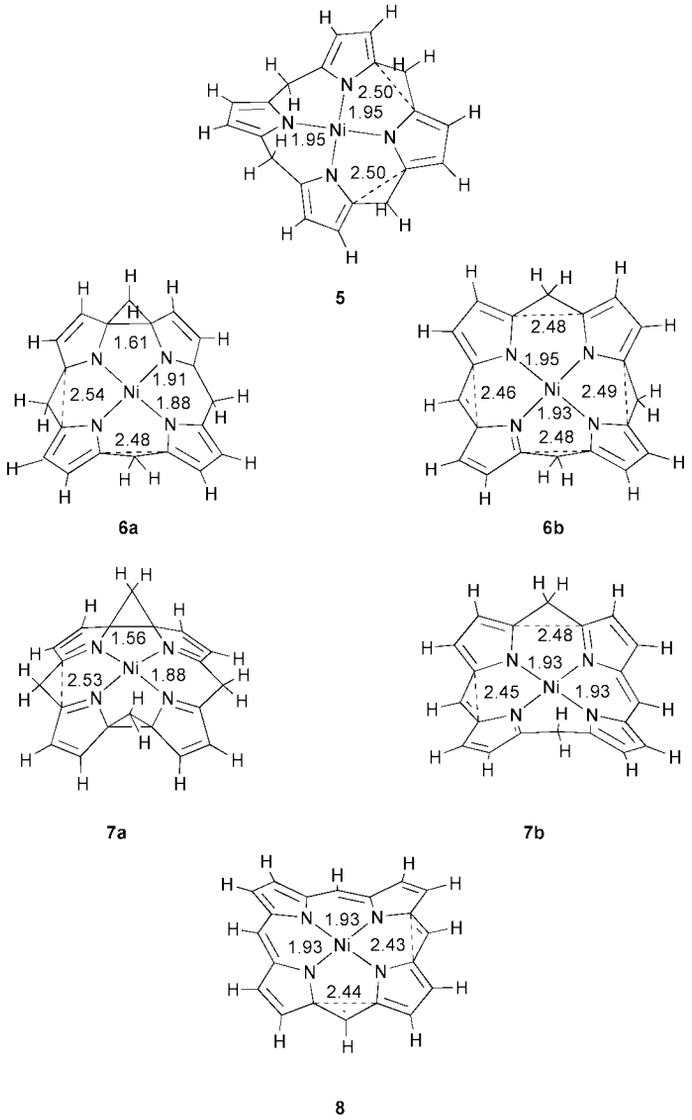

Fig. 2 Optimized structure of $[H_8N_4Ni]^{2-}$ (species **5**), $[H_8N_4(\triangle)Ni]$ (**6a**), $[H_7N_4Ni]^{-}$ (**6b**), $[H_8N_4(\triangle_2)Ni]^{2+}$ (**7a**), $[H_6N_4Ni]$ (**7b**), $[H_4N_4Ni]$ (**8**). Details as in Fig. 1.

Table 3 Energetics for the metal complexes in the unconventional and conventional routes and relative stability of the intermediate species. Energies in kcal mol^{-1}

	ΔE	
Step	M = Ni	Co
5 ⟶ **6a**	79	78
5 ⟶ **6b** + H^-	38	37
6a ⟶ **7a**	365	365
6b ⟶ **7b** + H^-	106	105
7a ⟶ **8** + H_2	−239	−245
7b ⟶ **8** + H_2	7	3
Relative stability		
6a ⟶ **6b**	−14	−15
7a ⟶ **7b**	−246	−248

overlooked, and this generates the discrepancy between the theoretical forecast and what is experimentally found. The metal-containing forms in Scheme 2 are anionic and the calculations do not take into account the important energy contribution to the stepwise reaction coming from the solvation of the counter cations by the solvent and the porphyrinogen itself. In many such derivatives the counter cation is η^3, η^5 strongly bound to the pyrrolyl anions. The anomalous instability of **7a** can be associated to the factors mentioned above and to the fact that Ni was used, while the derivatives have experimentally been observed in the case of Mn, Fe, and Co. In the latter cases the presence of a metal–halogen bond and the lower cationic charge may be important thermodynamic contributions to the stability of the bis(cyclopropane) derivative. However, even the cobalt complex of type **7a** without the apical halogen atom is very unstable. Indeed, the stabilization due to the coordination of, for instance, Cl^- is as high as 187.9 kcal mol^{-1}. The unconventional pathway **a** (Scheme 2) is even more "jumping"-like than the free ligand case, for the reasons mentioned above.

The energetics of the two possible oxidation processes from porphyrinogen to porphyrin through pathway **a** and **b**, for the free ligand and for the metal complexes, is shown in a graphical form in Fig. 3, considering only the total energies of the investigated species and excluding the contribution by the counter cations in Scheme 2. A similar smoother trend for pathway **b** has been observed in both cases (Schemes 1 and 2). The much higher instability of species **a** *vs.* **b** is consistent with the experimentally observed conversion of **6a** and **7a** into **6b** and **7b**, respectively.

Conclusion

The DFT calculations allowed the evaluation of the energetics for the two possible stepwise oxidation pathways, **a** and **b**,

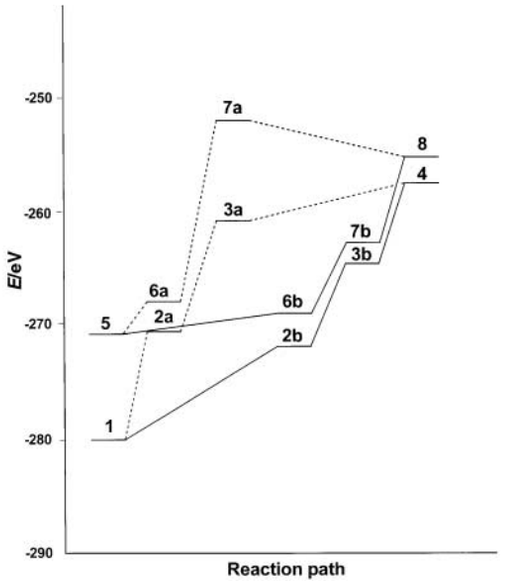

Fig. 3 Energy differences (eV) for the unconventional and conventional oxidation of porphyrinogen to porphyrin with and without the metal.

leading from porphyrinogen to porphyrin. They have been analyzed both in the case of the metal-free and of the metal-containing form of the porphyrinogen skeleton, with a quite coherent result indicating that pathway **b** (Schemes 1 and 2) passing through the intermediate formation of porphodimethene (5,15-dihydroporphyrin) (**3b**, **7b**) is the energetically preferred one. The presence of the metal did not modify the general energy trend of the entire process, though in the case of pathway **b** (Scheme 2) some major energy contributions, associated to the solvation of the counter cation, have probably been overlooked. A more complete analysis, taking care of those contributions and the role played by the transition metal ions undergoing, unlike nickel, changes in the oxidation state, is planned for the future.

Acknowledgements

The present work has been carried out within the Italian National Research Council (CNR) "Progetto Finalizzato Materiali Speciali per Technologie Avanzate II".

References

1 C. Floriani and R. Floriani-Moro, in *The Porphyrin Handbook*, eds. K. M. Kadish, K. M. Smith and R. Guilard, Academic Press, Burlington, MA, 1999, vol. 3; ch. 24, pp. 385–403 and references therein; ch. 25, pp. 405–420 and references therein.
2 *Porphyrins and Metalloporphyrins*, ed. K. M. Smith, Elsevier, Amsterdam, 1975; *The Porphyrins*, ed. D. Dolphin, Academic Press, New York, 1978; T. Mashiko and D. Dolphin, in *Comprehensive Coordination Chemistry*, eds. G. Wilkinson, R. D. Gillard and J. A. McCleverty, Pergamon, Oxford, 1987, vol. 2, ch. 21.1, p. 855.
3 S. De Angelis, E. Solari, C. Floriani, A. Chiesi-Villa and C. Rizzoli, *J. Am. Chem. Soc.*, 1994, **116**, 5702.
4 S. De Angelis, E. Solari, C. Floriani, A. Chiesi-Villa and C. Rizzoli, *J. Am. Chem. Soc.*, 1994, **116**, 5691.
5 R. Crescenzi, E. Solari, C. Floriani, A. Chiesi-Villa and C. Rizzoli, *J. Am. Chem. Soc.*, 1999, **121**, 1695.
6 L. Bonomo, E. Solari, R. Scopelliti, C. Floriani and N. Re, *J. Am. Chem. Soc.*, 2000, **122**, 5312.
7 M. Rosi, A. Sgamellotti, F. Franceschi and C. Floriani, *Chem. Eur. J.*, 1999, **5**, 2914.
8 See for example: C. W. Bauschlicher, A. Ricca, H. Partridge and S. R. Langhoff, in *Recent Advances in Density Functional Theory*, ed. D. P. Chong, World Scientific Publishing Co., Singapore, 1997, Part II.
9 E. J. Baerends, D. E. Ellis and P. Ros, *Chem. Phys.*, 1973, **2**, 42.
10 E. J Baerends and P. Ros, *Chem. Phys.*, 1973, **2**, 51.
11 E. J. Baerends and P. Ros, *Int. J. Quantum Chem.*, 1978, **S12**, 169.
12 W. Kohn and L. Sham, *J. Phys. Rev. A*, 1965, **140**, 1133.
13 S. H. Vosko, L. Wilk and M. Nusair, *Can. J. Phys.*, 1980, **58**, 1200.
14 D. M Ceperley and B. J. Alder, *Phys. Rev. Lett.*, 1980, **45**, 566.
15 A. D. Becke, *Phys. Rev. A*, 1988, **38**, 3098.
16 J. P. Perdew, *Phys. Rev. B*, 1986, **33**, 8822; J. P. Perdew, *Phys. Rev. B*, 1986, **34**, 7406.
17 P. M. Boerrigter, G. te Velde and E. J. Baerends, *Int. J. Quantum Chem.*, 1988, **33**, 87.
18 G. te Velde and E. J. Baerends, *J. Comput. Phys.*, 1992, **99**, 84.
19 We use the symbol △ to denote the cyclopropane ring in analogy with the notation used for the experimental systems.[4]